Optical spectroscopy of $PrTiNbO_6$, $NdTiNbO_6$ and $ErTiNbO_6$ single crystals

1996 J. Phys.: Condens. Matter 8 4837

(http://iopscience.iop.org/0953-8984/8/26/015)

J. Phys.: Condens. Matter **8** (1996) 4837–4845. Printed in the UK

Optical spectroscopy of $PrTiNbO_6$, $NdTiNbO_6$ and $ErTiNbO_6$ single crystals

X Qi, T P J Han, H G Gallagher, B Henderson, R Illingworth and I S Ruddock

Department of Physics and Applied Physics, University of Strathclyde, Glasgow G1 1XN, UK

Received 19 January 1996, in final form 28 March 1996

Abstract. The optical absorption and photoluminescence properties of $PrTiNbO_6$, $NdTiNbO_6$ and $ErTiNbO_6$ crystals grown by laser-heated pedestal growth (LHPG) have been measured at $T = 14$ K, 77 K and 300 K. These spectra show very high absorption coefficients for the three rare-earth (RE) ions and strong luminescence signals characteristic of ions at high concentration in distorted symmetry sites. The rare-earth ions in these compounds are shown to occupy single sites only. The strong luminescence output at 300 K makes these crystals potential hosts for diode-pumped laser gain media.

1. Introduction

The stoichiometric rare-earth compounds NdP_5O_{14}, $LiNd(PO_3)_4$, $K_3Nd(PO_4)_2$ and $NdAl_3(BO_3)_4$ have all been used as gain media in solid-state lasers [1, 2]. These compounds have high concentrations of rare-earth ions ($\simeq 3\times 10^{21}$ cm^{-3}) intrinsic to the crystal structure and large absorption and emission cross sections which suggest potential applications in diode-pumped solid-state lasers. Since the absorption lines of Nd^{3+} in these compounds are rather narrow ($\sim$1 nm) they are not optimally matched to the output of conventional laser diodes at $\simeq$810 nm which have linewidths of about 2–3 nm. Much current research on diode-pumped lasers seeks to improve the tolerance of the gain medium to the pump wavelength by designing materials with broader absorption lines.

The stoichiometric $RETiNbO_6$ crystals, in which RE represents lanthanide rare-earth ions with atomic numbers in the range 57–63 (i.e. La^{3+} to Eu^{3+}) in the periodic table, crystallize in the orthorhombic aeschynite structure with space group *Pnma* and four formula units per unit cell [3]. The oxygen coordination polyhedra of Nb(Ti) ions in these crystals are distorted octahedra joined in pairs by edge sharing, each pair being connected to six other pairs by corner sharing. The RE^{3+} ions occupy interstitial sites in the three-dimensional network where they are coordinated to eight O^{2-} ions, the RE–O distances all being of slightly different lengths. The RE polyhedra are connected by edges into chains along the [010] direction, the RE–RE distances being $\sim$0.39 nm along the chain and $\sim$0.60 nm between the chains. $RETiNbO_6$ crystals have the aeschynite or euxenite structure when the RE atomic number is in the range 64–71 (i.e. Gd^{3+} to Yb^{3+}), depending on the mode of preparation [4]. The euxenite crystal structure is also orthorhombic with four formula units per unit cell and belongs to the *Pbcn* space group [3]. The oxygen coordination polyhedra of $Nb(Ti)O_6$ are also distorted octahedra but in this structure are joined by edge or corner sharing to form a double layer perpendicular to the *c*-axis. The RE^{3+} ion is eightfold coordinated

0953-8984/96/264837+09$19.50

with O^{2-} at a site with C_2 symmetry. Each of the REO_8^{13-} polyhedra edges shares with four others forming a single layer which divides neighbouring $Nb(Ti)O_6$ double layers. The RE^{3+}–RE^{3+} separations within the RE–O layer are at slightly different distances of 0.375 nm or 0.385 nm, whereas the minimum separation between RE^{3+} and RE^{3+} between the layers is $\simeq$0.78 nm. Recently the authors reported the growth of miniature single crystals of $PrTiNbO_6$ (PTN), $NdTiNbO_6$ (NdTN) and $ErTiNbO_6$ (ETN) by laser-heated pedestal growth (LHPG) [5], when the ETN crystals have the euxenite structure.

This paper discusses the optical spectra of Pr^{3+} ($4f^2$), Nd^{3+} ($4f^3$) and Er^{3+} ($4f^{11}$) in these $RETiNbO_6$ crystals (see table 1).

Table 1. Structures and unit-cell parameters of some $RETiNbO_6$ compounds.

Compound	Structure	Space group	Unit-cell parameters (Å)			RE^{3+} concentration (10^{21} cm^{-1})
			a	*b*	*c*	
$PrTiNbO_6$	Aeschynite	*Pnma*	10.99	7.532	5.377	9.0
$NdTiNbO_6$	Aeschynite	*Pnma*	10.99	7.511	5.357	9.1
$ErTiNbO_6$	Euxenite	*Pbcn*	14.58	5.542	5.185	9.5

2. Experimental methods

The LHPG technique was used to grow mini-crystals (10 mm $\times$ 0.5 mm Ø) of PTN, NdTN and ETN [5]. Laue x-ray diffraction showed the minicrystals to have single-crystal structure, although they were randomly orientated. They were mechanically and chemically stable, showed no cleavage facets and were insoluble in water and in nitric acid. The as-grown crystals were opaque and black in colour. After annealing for eight hours in air at 1550 K they became transparent and coloured. The annealed NdTN was dark red, PTN crystal was emerald green and ETN crystal was pink. X-ray diffraction studies confirmed that the as-grown and the annealed crystals had the same structure, implying that the colour changes are not due to structural modifications. Similar changes in other oxides (e.g. TiO_2 and TGS) have been shown to be due to oxygen deficiencies in the as-grown crystal [6].

Experimental samples were in the form of single-crystal rods with typical diameter 0.5 mm fixed with pitch into a brass collar, where the end surfaces could be ground and polished on diamond-impregnated laps to a high-quality finish. Samples with typical thicknesses of 0.3–0.5 mm were used in optical absorption (OA) measurements. Photoluminescence (PL) measurements were made on samples $\simeq$2.0 mm thick, fixed into a copper holder and immersed in liquid nitrogen. Input and output beams were guided to and from samples by optical fibres, which have flat optical responses across the wavelength ranges of interest.

The OA measurements were made using a single-beam spectrophotometer at temperatures of 77 K and 300 K. White light from a tungsten lamp (12 V, 45 W) was focused onto the sample through the slots in an electromechanical chopper, which also provided the reference signal for a lock-in amplifier. The transmitted radiation was collected by a microscope objective and directed onto the entrance slit of a monochromator. The intensity of transmitted radiation at a particular wavelength was then measured at the exit slit using either a Si photodiode (NIR region) or photomultiplier tube (visible region). The transmitted light signal, modulated at the chopper frequency, was amplified by a lock-in amplifier and stored digitally in a microcomputer. This signal was converted to the optical density

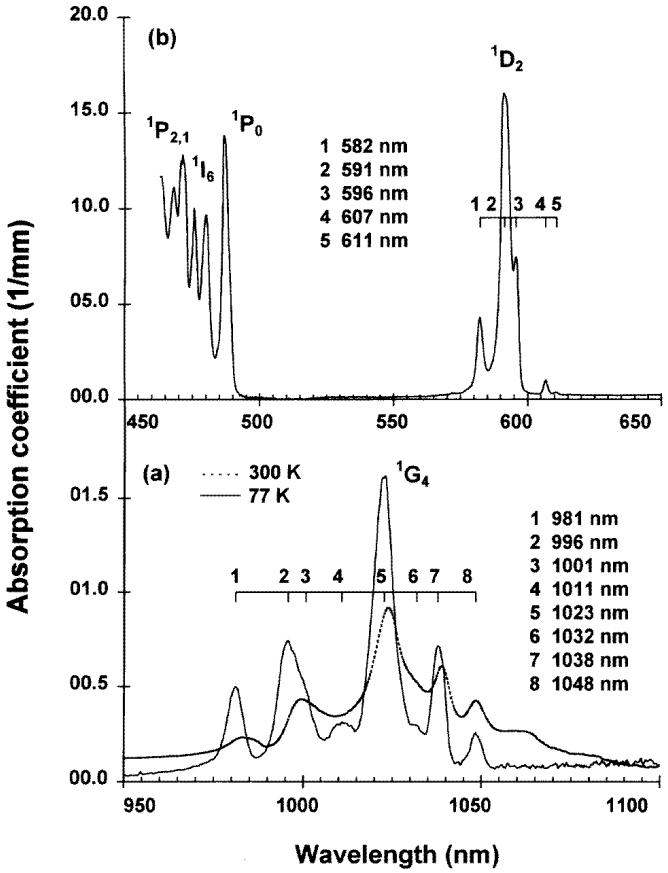

Figure 1. The optical absorption spectra of Pr^{3+} ions in PTN measured at 77 K for the (a) $^1G_4$ and (b) $^1P_0$ and $^1D_2$ multiplets.

$I(\nu)/I_0(\nu)$ by the computer, which contained information on $I_0(\nu)$ recorded by the system in the absence of the sample. To record the PL spectra the tungsten lamp was replaced by an Ar^+ laser. Filters were placed between the Ar^+ laser and the chopper to remove traces of discharge radiation and between the microscope objective and the entrance slit of the monochromator to absorb excitation light from the Ar^+ laser.

3. Experimental results

Optical absorption spectra of Pr^{3+} in PTN at 77 K are shown in figure 1. In the wavelength range 970–1070 nm, figure 1(a), eight components of the $^3H_4 \rightarrow {}^1G_4$ transition split by the electrostatic crystal field are indicated. The weak line at 1082 nm in the spectrum recorded at 300 K, also shown in figure 1(a), is due to a transition from the second-lowest crystal-field level of $^3H_4$, which has a significant thermal population at this temperature. Figure 1(b) shows the absorption spectrum at 77 K measured in the wavelength range 450–650 nm: there are five lines near 590 nm from the $^3H_4 \rightarrow {}^1D_2$ transition, a single line at 490 nm due to the $^3H_4 \rightarrow {}^3P_0$ transition as well as transitions from the $^3H_4$ ground term to $^1I_6$ (at 480 nm), $^3P_1$ (476 nm) and $^3P_2$ (472 nm). The crystal-field splittings of

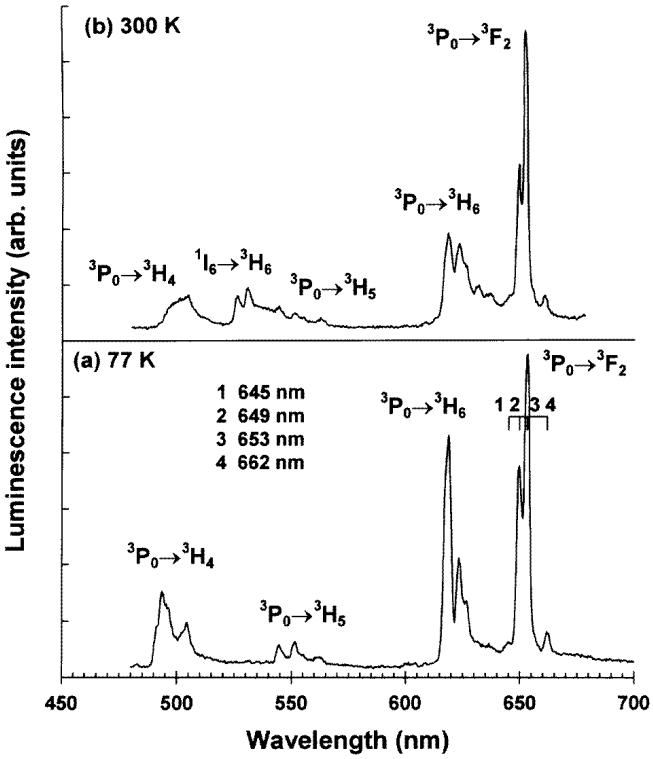

Figure 2. Photoluminescencespectra of Pr^{3+} ions in PTN measured at (a) 77 K and (b) 300 K.

the $^1I_6$, $^3P_1$ and $^3P_2$ levels are too small to resolve on this scale. PL spectra of PTN excited at 77 K and 300 K using an Ar^+ laser are shown in figure 2. The strong lines at $\simeq$650 nm and $\simeq$620 nm are due to the electric-dipole-allowed $^3P_0 \rightarrow {}^3F_2, {}^3H_6$ transitions, respectively [7, 8]. The $^3P_0 \rightarrow {}^3H_6$ transition is much weaker at 300 K relative to the $^3P_0 \rightarrow {}^3F_2$ transition than at 77 K. The normally forbidden $^3P_0 \rightarrow {}^3H_5$ PL spectrum is weakly observed at $\simeq$550 nm. Also observed at 300 K are the $^1I_6 \rightarrow {}^3H_6$ lines at 530 nm due to thermal promotion from the $^3P_0$ level to $^1I_6$. Weak $^3P_0 \rightarrow {}^3H_5$ lines are also observed centred at 500 nm. In general, the lines are rather broader at 300 K than at 77 K, so individual components are more difficult to isolate. At 77 K the lines are still quite broad and not all lines from particular manifolds are resolved. For example, at low temperature the $^3P_0 \rightarrow {}^3F_2$ transition should display five components due to the removal of the fivefold degeneracy of the $^3F_2$ level. Only four levels are identified in the spectrum. Both of the transitions $^3P_0 \rightarrow {}^3F_2$ (650 nm), $^3H_6$ (620 nm) are strong, whereas the $^3P_0 \rightarrow {}^3H_4, {}^3H_5$ and $^1I_6 \rightarrow {}^3H_6$ transitions are quite weak.

Figure 3(a) shows the OA spectrum of NdTN in the range 400–900 nm measured at 77 K. The absorption coefficient of the lines near 805 nm is $\simeq$170 cm^{-1}, with a FWHM of 35 cm^{-1} (or 2.5 nm). These lines are due to the overlapping transitions $^4I_{9/2} \rightarrow {}^2H_{9/2}, {}^4F_{5/2}$. Some groups of lines are quite complex especially those near 580 nm which are associated with the almost degenerate $^2G_{7/2} + {}^4G_{5/2}$ levels. The luminescence spectrum of NdTN measured at 77 K is shown in figure 4(a) to consist of two sets of lines, originating on the lowest-lying $^4F_{3/2}$ level and corresponding to the $^4F_{3/2} \rightarrow {}^4I_{9/2}$ and $^4I_{11/2}$ transitions. There are five

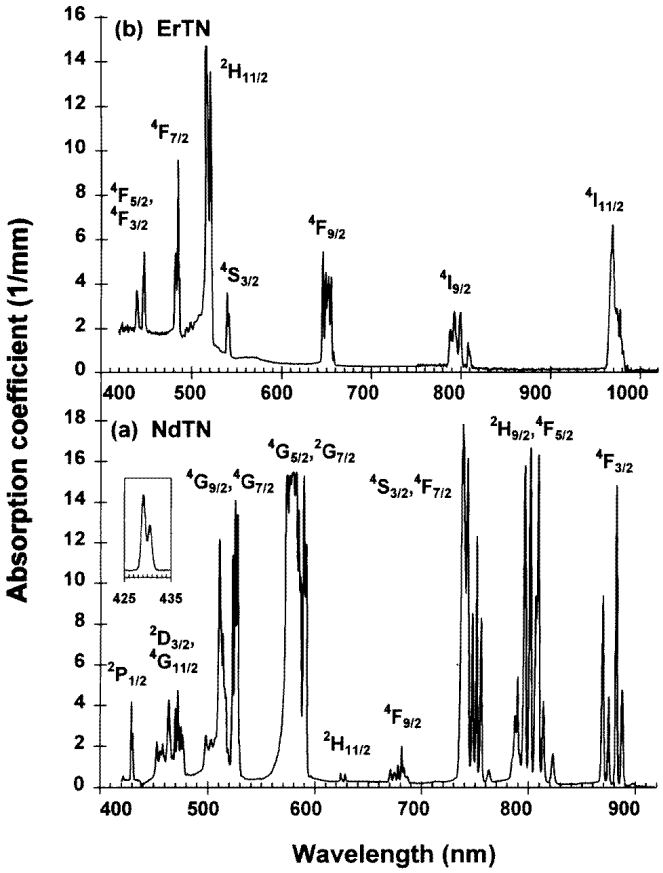

Figure 3. Optical absorption spectra of (a) Nd^{3+} ions in NdTN and of (b) Er^{3+} ions in ETN, measured at 77 K.

well-resolved lines due to the crystal-field splitting of $^4I_{11/2}$ and five from transitions into $^4I_{9/2}$. Although only vestiges of the luminescence from the higher-lying level of the $^4F_{3/2}$ manifold remain at 77 K, lines from both components of $^4F_{3/2}$ are present when measured at 300 K.

When grown by LHPG, ETN crystals have the euxenite structure. The OA spectrum of Er^{3+} in ETN over the wavelength range 420–920 nm and measured at 77 K (figure 3(b)) shows a large number of well-resolved lines, indicating that the Er^{3+} ions are isolated from each other in the euxenite structure. Transitions are observed from $^4I_{15/2}$ up to $^4I_{11/2}$ (970 nm), $^4I_{9/2}$ (800 nm) and all other levels up to $^4F_{3/2,5/2}$ (445 nm). The five crystal-field components of the $^4I_{15/2} \rightarrow {}^4I_{9/2}$ transitions centred at 800 nm and $^5I_{15/2} \rightarrow {}^4F_{9/2}$ transitions near 650 nm are resolved. Two components of the $^4I_{15/2} \rightarrow {}^4S_{3/2}$ transition are observed centred at 540 nm. Other transitions show overlap of the individual lines such that they are poorly resolved. OA measurements at $T = 300$ K show weaker spectra from absorption transitions originating on higher-lying, thermally populated crystal-field levels of the $^4I_{15/2}$ ground multiplet. The PL spectra of Er^{3+} in ETN were measured in the wavelength range 500–900 nm. There is very strong emission from the lowest crystal-field level of $^4S_{3/2}$ to the various components of the $^4I_{15/2}$ multiplet. Also shown are weaker

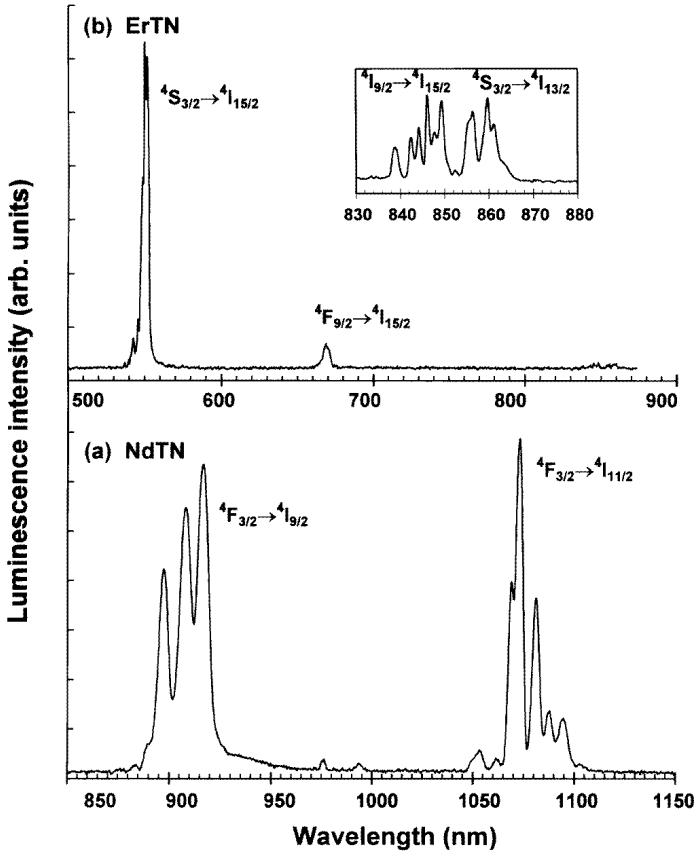

Figure 4. Photoluminescence spectra (a) Nd^{3+} ions in NdTN and (b) Er^{3+} ions in ETN, measured at 15 K.

signals due to the $^4F_{9/2} \rightarrow {}^4I_{15/2}$ transition at 670 nm, $^4S_{3/2} \rightarrow {}^4I_{13/2}$ at 845 nm and $^4I_{9/2} \rightarrow {}^4I_{15/2}$ at 850 nm. The response of the photodetector used to collect these spectra is primarily responsible for the differences in intensities of the spectra near 670 nm and 840–870 nm relative to the $^4S_{3/2} \rightarrow {}^4I_{15/2}$ transitions.

4. Discussion

The stoichiometric lanthanide compounds $RETiNbO_6$ used in this study crystallize with the aeschynite (PTN, NdTN) or euxenite (ETN) crystal structures, where the principal difference between the RE^{3+} sites is that they lie in closely connected chains in aeschynite and densely packed parallel planes in euxenite. The very high concentrations of lanthanide ions in these compounds, $\simeq 10^{22}$ cm^{-3} in each case, are 2–3 times larger than those in other rare-earth compounds used in solid-state lasers. Such strong absorptions suggest that rather short absorption lengths of these rare-earth compounds are of potential application as gain media in microlasers.

The spectra of rare-earth ions such as Pr^{3+} ($4f^2$), Nd^{3+} ($4f^3$) and Er^{3+} ($4f^{11}$) are composed of rather sharp lines as a consequence of the $4f^n$ electrons being shielded by the

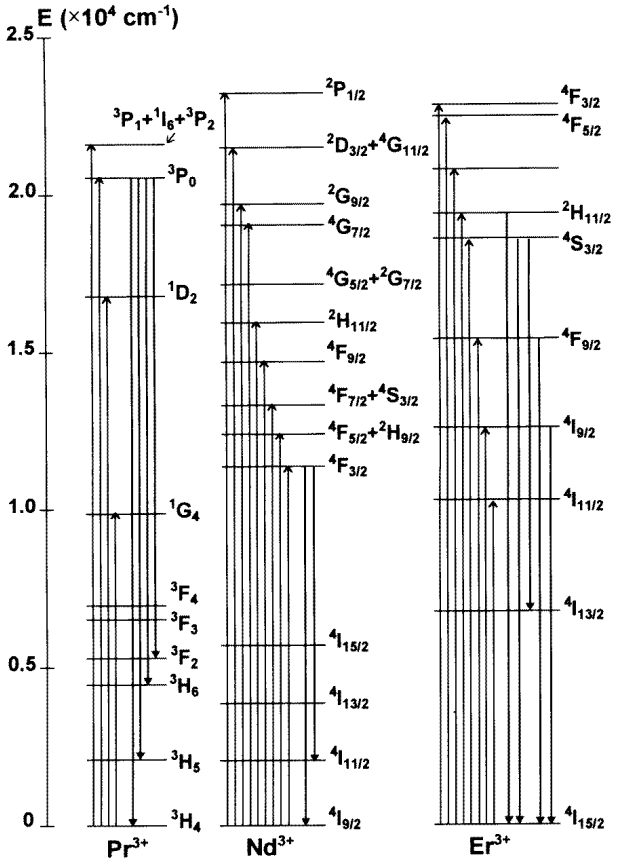

Figure 5. The energies of the free-ion levels of Pr^{3+}, Nd^{3+} and Er^{3+} in RETN crystals and the absorption and photoluminescence transitions identified in the present study.

outer 5s and 5p shells of electrons. Neglecting interactions with the electrostatic crystal field, the energy levels of the $4f^n$ electrons are just the free-ion levels characterized by the quantum numbers L, S and J in the Russell–Saunders coupling approximation. The REO_8^{13-} polyhedra are distorted by both even- and odd-parity displacements of ligand ions. Even parity displacements of the ligand ions split the free-ion levels by amounts determined by the strength and symmetry of the electrostatic field at the RE^{3+} site. The number of crystal-field levels that a given free-ion J-value splits into is determined from group theory. Accordingly, the $(2J + 1)$-fold degeneracy of an integral J-value free ion is fully raised by crystal-field symmetries lower than D_3, whereas for odd half-integer J-values the degeneracies are removed for all symmetries lower than octahedral, except the twofold Kramers degeneracy. In general, the crystal-field splitting of the free-ion levels of the trivalent lanthanide ion is much less than the separations of the free-ion levels, so the gross features of rare-earth-ion spectra vary little from host crystal to host crystal although the *crystal-field splittings* may vary markedly. In consequence, the optical spectra of RE^{3+} in crystals are composed of groups of narrow crystal-field lines approximately centred on the positions of the lines observed in free-ion spectra. The observed spectra in figures 1 and 4 may then be interpreted using the partial energy level diagram in figure 5, in which only

the free-ion levels of Pr^{3+}, Nd^{3+} and Er^{3+} are shown as well as the identified absorption and emission transitions.

In principle, $4f^n \leftrightarrow 4f^n$ transitions of RE^{3+} are forbidden by the Laporte selection rule. However, the selection rule is partially lifted in crystals by odd-parity crystal-field distortions which mix opposite-parity wavefunctions into the $4f^n$ wavefunctions of the RE ion. The specific nature and positions of these opposite-parity states are not known. Judd [7] and Ofelt [8] assumed that the unoccupied $4f^{n-1}$ 5d levels were involved although these were some 3–4 eV higher in energy than the $4f^n$ levels. Given the presence of ligand hyperfine structure in ESR spectra of RE ions in crystals it is probable that overlaps of the $4f^n$ levels with ligand 2s and 2p orbitals also contribute, and these are much closer in energy [9]. Such covalent spin transfer has been discussed for the cases of Ti^{3+} and Cr^{3+} in laser hosts and shown to account accurately for the intensities and polarizations of the observed absorption and luminescence processes [10]. It is the low symmetry of the RE sites in $RETNbO_6$ crystals combined with the high RE concentrations that lead to the very strong line spectra in absorption and luminescence, and which encourage an expectation of efficient laser action. In general, the relative absorption intensities of the intermanifold transitions of Pr^{3+}, Nd^{3+} and Er^{3+} are in accord with theoretical expectations [7–9].

Consider now the spectra of Pr^{3+} in euxenite-PTN, where the PrO_8^{13-} polyhedra have C_2 symmetry [3]. In principle, the $^3H_4 \rightarrow {}^1G_4$ absorption is spin forbidden, but it becomes partially allowed by the Judd–Ofelt mechanism [7, 8]. According to group theory in C_2 symmetry the ninefold degeneracies of both $^3H_4$ and $^1G_4$ levels are fully removed. Assuming that at 77 K only the lowest crystal-field level of $^3H_4$ is thermally occupied the *nine* absorption lines from the $^3H_4 \rightarrow {}^1G_4$ transition are expected. Careful examination of the $^3H_4 \rightarrow {}^1G_4$ spectrum in figure 1(a) suggests eight overlapping components. The $^3H_4 \rightarrow {}^1D_2$ absorption spectrum at 77 K consists of five lines, figure 2(b), due to the removal of orbital degeneracy of the $^1D_2$ state by the crystal field. The $^3P_0$ level is not split by the crystal field and only a single line is observed in figure 2(b) at 77 K and 300 K.

The interest in developing Pr^{3+}-containing crystals as solid-state laser gain media follows from the Stark splitting of the free-ion levels which permits so many allowed transitions in low-symmetry hosts. More than twenty laser transitions have been identified in Pr^{3+}-doped materials ranging from the blue to mid-infrared spectral regions. Sandrock *et al* [12] observed efficient laser operation for six wavelengths in Pr^{3+}:YLF at room temperature. Subsequently Sutherland *et al* [13] recorded a further fourteen laser channels in this host! One important laser transition is $^3P_0 \rightarrow {}^3H_6$, the efficiency of which is determined by nonradiative decay from $^3P_0$ to the $^1D_2$ level. The $^3P_0 \rightarrow {}^1D_2$ energy gap is $\simeq$3600 cm^{-1} in PTN. The relative intensities of the $^3P_0 \rightarrow {}^3H_6$ lines at 77 K and 300 K in figure 2 demonstrate that nonradiative decay is important in PTN, although not necessarily sufficient to quench laser action at room temperature.

Both Nd^{3+} ($4f^3$) and Er^{3+} ($4f^{11}$) have half-odd-integer J-values. In consequence, when occupying the Re^{3+} sites in $RETiNbO_6$ all free-ion levels have all degeneracies removed, other than the Kramers degeneracy. For Nd^{3+} the different LS-terms spanning the energy range to 25 000 cm^{-1} are $^4I, {}^4F, {}^4S, {}^2H, {}^2G, {}^4G, {}^2D$ and ^2P in order of increasing energy. The ground term ^4I is split by spin–orbit coupling into $J = \frac{9}{2}, \frac{11}{2}, \frac{13}{2}$ and $\frac{15}{2}$ with $^4I_{9/2}$ being the ground multiplet. This multiplet is split by crystal-field interaction into five levels, and optical absorption transitions at low temperature are observed only from the lowest-energy crystal-field level. The luminescence spectrum of Nd^{3+} in NdTN, figure 4(a), was measured only in the wavelength range 850–1150 nm where transitions from the lowest crystal-field level of the $^4F_{3/2}$ multiplet to the $^4I_{9/2}$ and $^4I_{11/2}$ are observed. Even at 77 K the linewidths are very broad being typically 5 nm at the half-peak height. At 300 K the linewidths are

some 50% broader, and lines from the upper crystal-field level of the $^4F_{3/2}$ multiplet are also observed.

The optical spectra of Er^{3+} in ETN may be similarly interpreted to those of Nd^{3+} except that the spin–orbit coupling constant is negative, so multiplets occur in the opposite order. This is evident from the $^4I_{15/2} \rightarrow {}^4F_J$ multiplets, where $^4F_{3/2}$ multiplet is some 7000 cm^{-1} *above* $^4F_{7/2}$ in energy, although significant deviations from the Landé interval rule are apparent. The crystal-field splittings of the multiplets are quite small, so in general the different crystal-field lines are not resolved. Nevertheless, the five components of the $^4I_{15/2} \rightarrow {}^4F_{9/2}, {}^4I_{9/2}$ transitions are seen as are two components in the $^4I_{15/2} \rightarrow {}^4S_{3/2}$ spectrum.

Generally, the optical absorption and luminescence spectra of PTN, NdTN and ETN are very intense consequent on the high concentrations of RE ions in the crystals and the odd-parity distortions which enhance transition rates. The peak absorption coefficients in these crystals are in the range 150–180 cm^{-1} corresponding to absorption cross sections of around 10^{-18} cm^2. The absorption lines in each of the compounds are broad, typically 5–10 nm, suggesting that these stoichiometric rare-earth compounds have potential in the field of diode-pumped solid-state lasers. The large linewidths, in part, derive from the intrinsic disorder in structures in which half of the Nb ions in the NbO_6 octahedra are replaced by Ti ions. Such disorder contributes to the inhomogeneous broadening of the Re^{3+} crystal-field spectra. The large number of visible-region laser-active transitions [11, 12] may be pumped using the 476/488 nm lines of Ar^+ to access the ^3P_J levels of Pr^{3+} or by pumping the $^3H_4$–$^1D_2$ band near 590 nm with a Xe flashlamp. In contrast, both Nd^{3+} and Er^{3+} may be pumped using diode lasers, Nd^{3+} at 790–820 nm and Er^{3+} at 980 nm or 1.53 μm. In these cases the large absorption linewidths are advantageous since it is not crucial to temperature stabilize the diode output wavelengths.

Acknowledgments

The authors are indebted to the EPSRC and MoD for their support of the experimental programmes via Research Grants GR/G/42051 and GR/K/04392. XQ is grateful to the CVCP for their award of an Overseas Research Studentship and the University of Strathclyde for their award of a John Anderson Research Scholarship.

References

[1] Weber M J (ed) 1982 *Lasers and Masers (Handbook of Laser Science and Technology 1)* (Boca Raton, FL: Chemical Rubber Company Press)
[2] Kaminskii A A 1990 *Laser Crystals* 2nd edn (Berlin: Springer)
[3] Aleksandrov V B 1963 *Dokl. Akad. Nauk* **142** 181
[4] Komkov A I 1963 *Dokl. Akad. Nauk* **148** 1182
[5] Qi X, Illingworth R, Gallagher H G, Han T P J and Henderson B 1996 *J. Cryst. Growth* **160** 111
[6] Weitzel H and Schröne H 1980 *Z. Kristallogr.* **152** 69
[7] Judd B R 1962 *Phys. Rev.* **127** 750
[8] Ofelt G S 1962 *J. Chem. Phys.* **37** 511
[9] Owen J and Thornley J M 1968 *Rep. Phys.* **29** 675
[10] Yamaga M, Henderson B and O'Donnell K P 1990 *J. Lumin.* **46** 397
[11] Kaminskii A A, Mironov V S, Bagaev S N, Boulon G and Djeu N 1994 *Phys. Status Solidi* b **185** 487
[12] Sandrock T, Danger T, Heumann E, Huber G and Chai B H T 1994 *Appl. Phys.* B **58** 149
[13] Sutherland J M, French P M W and Taylor J R 1996 at press